

Micro-Nano Photonics Building Thermal Insulation Material Based on Porous Material-Based Metal Dielectric Film

Anlli Teekarama*

Vrije Universiteit Brussel, Belgium

**corresponding author*

Keywords: Porous Materials, Dielectric Films, Micro-Nano Photonics, Thermal Insulation Materials

Abstract: Insulation materials are materials with a guiding thermal coefficient of less than or equal to 0.12. They are widely used in industry and construction. With the help of industry expertise, they can achieve a multiplier effect with half the effort. To a certain extent, the development of materials reflects the level of productivity development of the times, and its quality and output are important indicators to measure the level of scientific, technological and economic development of a country. This article aims to study the application of micro-nano photonics based on porous material-based metal dielectric films in the field of building insulation materials, and analyze the physical properties of dielectric films through related techniques, and conduct quasi-static analysis of the emerging waveguide structures. This paper proposes that glass powder is used as the main raw material, and porous materials are prepared by demagic technology and spray drying technology, and this material is a new choice for building insulation materials. Based on the life cycle of insulation materials and the model of investment cost, it is found that the energy consumption of insulation materials is the largest in the process of putting them into use, and the loss during transportation is the smallest. The experimental results show that when the temperature is between 650-660, the bulk density of the porous material decreases from 0.26 to 0.17. As the temperature continues to rise, the bulk density of the porous material reaches 0.15 at the lowest point, and the porosity is close to 94% at the highest temperature. When it is in the range of 650-660, the pressure drops rapidly, from 7.6 to 2.7.

1. Introduction

1.1. Background

In recent years, reports of fire accidents and pollution caused by the use of thermal insulation

materials are not uncommon. In order to solve these problems, new thermal insulation materials are imminent. Traditional thermal insulation materials mainly focus on increasing the gas porosity and reducing thermal conductivity and conductivity; fiber thermal insulation materials have higher requirements for convective and radiative heat transfer in the environment; profile-type inorganic thermal insulation materials need to be assembled and processed, and the loss is answered, With short service life, none of these insulation materials can become widely used materials. With the development of science and technology, the standards of electronic materials have been continuously improved, and the application of dielectric film materials has emerged. Dielectric film materials are currently widely used in the field of national defense and communications, and the materials are very thin, low loss, and high sensitivity. The use of dielectric film materials as a new type of thermal insulation material has become a current research hotspot. Porous materials have the characteristics of low density, high rigidity and strong adsorption. They can be used as materials in many fields, and can be used as heat insulation materials in the construction field, especially their low thermal conductivity characteristics. They are usually used as foam glass to prevent fires. . In view of the imperfection of current building insulation materials and the advantages of dielectric mold materials and porous materials in the construction field, we hope that through exploration, we can combine the advantages of these two materials to produce new building insulation materials.

1.2. Significance

Porous media widely exist in nature and human life. The use of new building insulation materials can reduce thermal bridges on the wall, protect the main structure of the building, and realize energy-saving transformation of the building; traditional building insulation materials have problems such as waste, excessive initial investment, and environmental protection. The new building insulation materials studied in this article It can be ignored that it is lost during transportation and installation, which reduces the waste of resources and greatly improves the environmental performance.

1.3. Related Work

Building insulation materials are an important manifestation of saving energy and improving the living environment. However, the existing building insulation materials have many problems and cannot fully solve the current problems. Therefore, the development of new building insulation materials is a general trend. Vanson J M proposed a computational model based on the lattice Boltzmann scheme to study the accessibility of active adsorption sites in hierarchical porous materials to the adsorbed substances in the flowing liquid in the pores. By studying the transport and adsorption of tracers after entering the pore space of the virtual sample, the kinetics when they pass through the pore space and adsorb on the solid-liquid interface are characterized. The model is verified on simple geometric figures with known analytical solutions. Then use it to study the influence of regular grooves or disordered roughness on the geometric wall of the slit hole, and to study the influence on adsorption and transport. The author particularly emphasizes the importance of the accessibility of adsorption sites, which depends on the shape and connectivity of the pore space, as well as the fluid flow profile and velocity [1].F Ebrahimi proposed a four-variable shear deformation refinement plate theory for free vibration analysis of embedded smart plates made of porous magneto-electroelastic functionally graded (MEE-FG) materials. It is assumed that the magneto-electroelastic properties of the FG plate vary in the thickness direction and are estimated by the modified power law rule, where the porosity of approximately uniform and non-uniform

types is approximated. Based on the four-variable tangential exponential refinement theory that avoids the use of shear correction factors, the control differential equations and boundary conditions of the embedded porous FG plate under the magnetic field are derived through the Hamiltonian principle. Analytical solution method is used to obtain the natural frequency of the embedded porous FG plate, assuming that it is a magnetic field with various boundary conditions [2]. Soare proposed that Gurson's method for studying the overall response of a rigid-plastic porous representative volume element (RVE) leads to a clear upper limit estimate only in a few specific cases, for example, when the matrix of RVE follows the quadratic rule (von Mises or Hill' 48). The difficulties in preventing GURSON's method from being applied to a wider range of materials, the current technical interest can be avoided by numerical methods, and the illustrations of the idealized rve in the form of hollow spheres with von Mises and Hershey hosford matrices are shown respectively. In both cases, the total yield surface is shown to have a complex geometry, the most notable feature is the change in the overall measurement of the equivalent stress along the pressure axis and the significant asymmetry of its level set in the range of the high triaxial S_{ex} [3]. Sadouki M proposed an enhanced ultrasound method to evaluate the acoustic parameters of air-saturated porous materials. This method is based on the front and back problem of oblique incident waves reflected from the surface of a rigid frame porous medium. The interaction between the acoustic pulse and the porous material is described by an equivalent fluid model, and the Johnson-Champoux-Allard method (JCA) is used to describe the viscous inertial dissipation effect and thermal effect inside the porous medium. The calculation of dynamic density and bulk modulus at high frequency involves four parameters, namely porosity ϕ , high frequency limit of curvature ∞ , viscosity and thermal characteristic length Λ and Λ' . For different oblique incident angles, the sensitivity of each parameter to the reflected wave from the surface of the porous medium is studied. The advantage of this method is that the inversion values of porosity, tortuosity, viscosity and thermal characteristic length are carried out simultaneously [4]. Hao JH theoretically analyzes the factors affecting the heat transfer performance of porous materials, such as temperature, pressure and porosity. Under the constraints of the quality and thickness of porous materials, the mathematical model is established by using the fire product theory. Finally, the governing equation for optimizing the distribution of porosity / solid fraction in porous materials is derived by using the variational principle. At the same time, one-dimensional and two-dimensional physical models are used as examples to demonstrate applications. When the surface temperature and the total mass and thickness of the high-porosity structure are given, we obtain the optimal porosity distribution by solving the newly derived governing equation. The results show that the heat flux and effective thermal conductivity of the optimized structure are the smallest [5]. Osorio J D studied the integration of transparent insulating materials (TIM) with flat plate collectors (FPC), parabolic trough collectors (PTC) and central receiver (CR) collectors. A general model including optical and thermal analysis was developed. The effects of TIM characteristics, such as emissivity, thermal conductivity, extinction coefficient and thickness, on the performance of the collector are analyzed. When the temperature of the absorber is low, the performance of the traditional collector is relatively high. Due to the increase in heat loss, the efficiency of these collectors will be significantly reduced at high temperatures. The addition of TIM reduces heat loss, thereby increasing the efficiency of the collector at high absorber temperatures. The main goal of this research is to determine the critical operating temperature, from which the reduction in heat loss overcomes the loss of light efficiency due to TIM integration. Generally speaking, for high-performance collectors, TIMs are characterized by low emissivity and thermal conductivity, high transmittance and low extinction coefficient [6]. Juan P has proposed a method to evaluate

"critical temperature", taking some of the most common insulation materials for buildings in the EU market as examples, namely rigid polyisocyanuric acid foam, rigid phenolic foam, rigid foamed polystyrene foam and low density flexible rock wool. The characterization of these materials is based on a series of specialized cone calorimeters and thermogravimetric experiments, helping to establish the basic principles behind critical temperature quantification. The temperature of the main peak of pyrolysis is obtained by differential thermogravimetric analysis at a low heating rate in a nitrogen atmosphere, and is proposed as the "critical temperature" for materials that do not shrink and melt significantly (ie, carbonized insulating materials). For materials with shrinkage and melting behavior, it is recommended to use the melting point as the "critical temperature". The recommended conservative values for "critical temperature" are 300 °C for polyisocyanurate, 425 °C for phenolic foam, and 240 °C for expanded polystyrene. The concept of "critical temperature" of low-density rock wool was examined in the same way, and it was found that it was not applicable because it could not promote combustible mixtures. In addition, the new method is used to obtain the thermal inertia value required by the performance-based method for PIR and PF, providing thermal inertia values in the range of 4.5 to $6.5 \times 10^3 \text{W}^2\text{sK}^2\text{m}^4$ [7]. Xu S designed and prepared a new ceramic composite thermal insulation material composed of alumina fiber and hollow silica powder, hereinafter referred to as (CCIM), which has excellent flexibility and thermal insulation properties. The effect of alumina fibers and hollow silica microspheres on the properties of composite materials was characterized by using scanning electron microscope (SEM) microstructure observation and thermal conductivity evaluation. In the new CCIM, ceramic fibers and particles of different sizes are uniformly mixed to form multi-scale pores, which can significantly reduce heat conduction and convection heat transfer at high temperatures. In this work, a comparison between traditional mineral wool and manufactured CCIM was also carried out, focusing on the microstructure and thermal insulation properties [8]. Although these theories have made a certain contribution to building insulation materials to a certain extent, their research is too ideal and not practical.

1.4. Innovation

In this paper, the heat and mass transfer model of the porous medium of the insulation material is established based on the rough macroscopic characterization volume element, and the mathematical model for the calculation of the thermal conductivity under different models is deduced, which provides a new idea for the research of the insulation material; Compared with the device, the operation is simple, the price is low, and it is easy to promote and use.

2. Micro-Nano Photonics Building Insulation Material Method Based on Porous Material-Based Metal Dielectric Film

2.1. Building Insulation Materials

Since the Third Plenary Session of the Eleventh Central Committee, China's economy has developed rapidly, and the construction field has also been improved to a great extent, but the backward technical level in the early stage of development caused a waste of resources [9]. Due to economic development and population base issues in recent years, China has become the world's largest energy consumer. Urban construction continues to deepen, the scale of the construction industry continues to expand, and the building area is growing at a rapid rate. The current building energy consumption accounts for one-third of the total energy consumption. According to this data,

under the current circumstances, less building energy consumption becomes a top priority. According to the data survey, the heat loss of the entire building is mainly composed of walls, doors and windows and roofs. The heat loss of doors and windows is 20%-30%, the heat loss of the roof is about 10%, and the heat loss of the wall is as high as 60%-70%. According to the data, it is not difficult to see that the energy saving of the wall has an important position in the entire building structure, and the use of high-efficiency insulation materials is of great significance to the entire construction industry, and is also the future development direction of the industry [10]. Figure 1 is a schematic diagram of common building insulation materials:

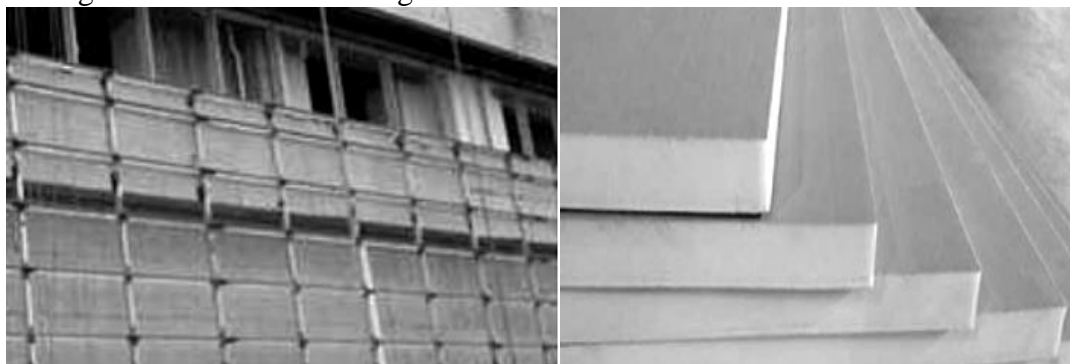


Figure 1. Common building insulation materials

Building insulation materials include organic insulation materials, inorganic insulation materials and other insulation materials. Organic thermal insulation materials have the advantages of light weight, strong thermal insulation and low price, and are widely used in sub-markets. However, organic thermal insulation materials have poor resistance and pose greater safety risks. Therefore, it is necessary to develop new thermal insulation materials [11].

Common organic insulation materials on the market include expanded polystyrene board, extruded polystyrene board, polyurethane and phenolic foam. Although they have advantages, their disadvantages cannot be ignored either. Although polyurethane is mature in production technology and has good thermal conductivity, its ignition point is low. Once it is burned, it will produce a large amount of harmful gases, which poses a threat to life safety and is also very harmful to the ecological environment. Although phenolic foam produces more harmful gases However, the strength of the material is low, the brittleness is too large, and the insulation effect is poor [12-13]. Table 1 shows the performance comparison of common organic thermal insulation materials.

The characteristics of organic thermal insulation materials determine its limitations as building materials. In addition, due to long-term ultraviolet radiation, rain erosion and other external environmental influences, the material life cycle is shortened, resulting in the loss of thermal insulation materials, which invisibly increases maintenance costs and Security cost [14].

The current inorganic thermal insulation materials on the market are mainly fiber, powder and rigid. Fibrous inorganic thermal insulation materials are mainly rock wool and glass wool. Among them, rock wool was first used as one of the inorganic thermal insulation materials. It has been developed into a complete system so far. However, due to the limitation of the material itself, the water absorption rate is relatively large. The thermal conductivity will increase rapidly, which will lead to a decrease in the insulation performance of the material. Glass wool has similar characteristics. When it absorbs water, it will deform, resulting in poor thermal insulation. However, glass wool is light in weight and good in sound absorption, so it can be used as a thermal insulation decoration material [15].

In addition to the thermal insulation materials described above, there are other thermal insulation materials on the market. Aerogel is a kind of ultra-light porous gel-like substance. It uses gas as a dispersion medium and has a nanostructure. It is currently the lightest material. Coupled with low density and large porosity, it is widely used in the fields of heat insulation and hydrogen storage [16].

Table 1. The performance of common organic thermal insulation materials

Organic insulation materials	Polyurethane	Phenolic foam	Polystyrene board
Thermal conductivity (W/m K)	0.021-0.035	0.029-0.035	0.03-0.04
Closed cell rate (%)	>85	35-45	>100
Density (kg/m ³)	23-39	40-90	10-50
Operating temperature (°C)	-100-100	-180-180	-80-80
Water absorption rate (%)	0.15	>3.5	1-2
Dimensional change rate (%)	≤2.2	≤1	≤3.2
Compressive strength (MPa)	0.1-0.2	0.15-0.2	0.1-0.16

2.2. Mechanical Theory of Porous Materials

The smallest unit of the porous material mentioned in this article is the cell body. These cell bodies are staggered internally to form different spatial structures. If the influence caused by the volume and mass of the material is ignored, the cell body and the relative density of the porous material [17]. The volume of space occupied by the cell body can be expressed by the following functional expression:

$$L = k^3 + 2i \quad (1)$$

Among them, L represents the volume, and k represents the length of the side length. The volume formula of the cell body matrix material can be expressed as:

$$L_c = k^3 - (k - 2i) = 2i(k^2 - 6ki + 4i^2) \quad (2)$$

Among them, L represents the volume, and k represents the length of the side length.

According to the above two volume formulas, we can express the relative density of porous materials as:

$$\phi = \frac{L_c}{L} = \frac{2i(k^2 - 6ki + 4i^2)}{k^3} \quad (3)$$

Among them, ϕ stands for density, and the other variables remain the same as above.

When the porous material is impacted, the thin-walled element will be under pressure, but according to the theory, the law of conservation of energy is still observed in this process, so when the porous material is under pressure, the external pressure will be transformed into the bending performance of the thin-walled element And film variable properties [18].

$$2kL_n\eta = W_z + W_i \quad (4)$$

Among them, k represents the half height of the folding unit, L_n represents the average stress of the folding unit being compressed, η represents the effective compression ratio, W_z represents the bending deformation energy, and W_i represents the variable performance of the film.

The functional expression of bending deformation energy is as follows:

$$W_z = 2\pi N_0 K_c \quad (5)$$

Among them, K_c represents the total length of the cell body used, N_0 represents the thin-walled plastic bending moment, and $N_0 = \frac{1}{4}\phi_0 c^2$.

Considering the strain hardening of porous materials in the calculation process, the flow stress value can be expressed by the following expression:

$$\phi_0 = \sqrt{\frac{\phi_a \phi_b}{1 + \lambda}} + \frac{1}{3}\phi_a c^2 \quad (6)$$

Among them, ϕ_a represents the yield strength of the base material, ϕ_b represents the ultimate strength of the base material, and λ represents the strain hardening coefficient. Figure 2 is a schematic diagram of the strain curve of porous materials:

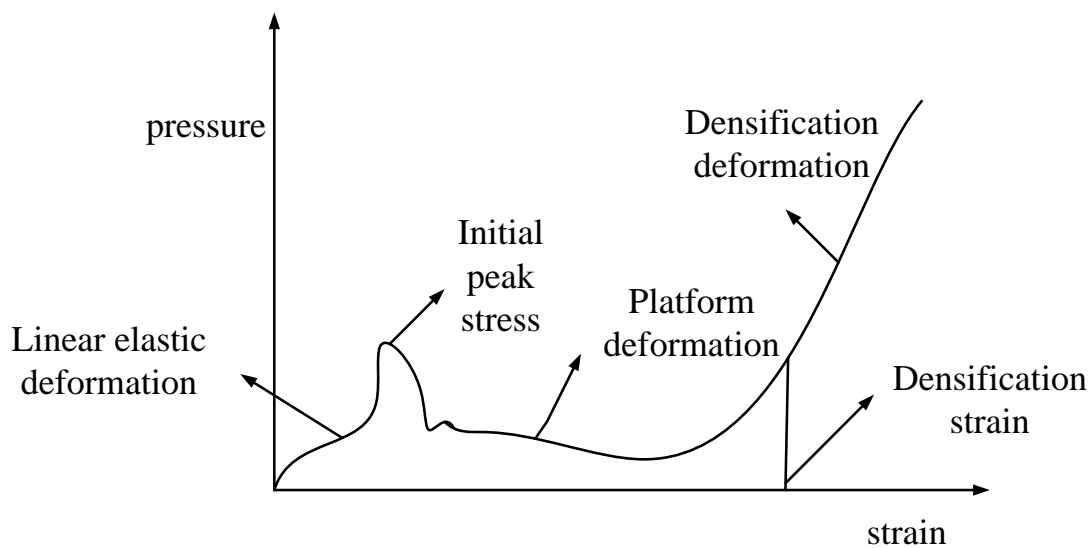


Figure 2. Strain curve of porous materials

Regarding the material model as a corner element, a cross-shaped element and a T-shaped element, the total film deformation properties of the three structures can be calculated by the compressed area during deformation.

The corner unit can be expressed as:

$$W_C = 2 \frac{1}{2} \phi_0 i k^2 = \frac{4N_0 k^2}{i} \quad (7)$$

The cross-shaped unit can be expressed as:

$$W_{CJ} = 4 \phi_0 i k^2 = \frac{16N_0 k^2}{i} \quad (8)$$

The T-shaped unit can be expressed as:

$$W_E = 2 \phi_0 i k^2 = \frac{8N_0 k^2}{i} \quad (9)$$

So we can get:

$$W_s = \frac{M_C W_C + M_{CJ} W_{CJ} + M_T W_T}{i} = \frac{(4M_C + 16M_{CJ} + 8M_T) N_0 K^2}{i} \quad (10)$$

Among them, M_C, M_{CJ}, M_T are the number of corner elements, cross elements and t-elements respectively.

We can get a simple summary of the listed function expressions:

$$0.71 \frac{L_n}{N_0} = 2(W_C + 4W_{CJ} + 2W_T) \frac{K}{i} + \pi \frac{L_t}{K} \quad (11)$$

Solving it can get:

$$k = \sqrt{\frac{\pi L_t i}{2(W_C + 4W_{CJ} + 2W_T)}} \quad (12)$$

$$L_n = \frac{2}{0.71} N_0 \sqrt{\frac{2(W_C + 4W_{CJ} + 2W_T) \pi L_t}{i}} \quad (13)$$

$$L_n = \phi_0 i \sqrt{(W_C + 4W_{CJ} + 2W_T) \pi L_t} \quad (14)$$

For porous materials, if $W_C = 4, W_{CJ} = (W - 1)^2, W_T = 4(W - 1), i = R/2(W - 1)\beta$, R represents the width of the porous material, the function expression can be used to obtain:

$$L_n = \sqrt{\pi} \phi_0 \frac{MR^{\frac{3}{2}}}{(W + 1)\beta} \quad (15)$$

When the number of cell bodies is not considered in the calculation process, we can express the function expression as:

$$L_n = \sqrt{\pi} \phi_0 \frac{R^{3/2}}{\beta} \quad (16)$$

The relative density of the structure can be expressed as $\delta = R/\alpha^2$, so

$$\phi_\delta = \frac{L_n}{\alpha^2} = \sqrt{\pi} \phi_0 \delta^{i-3/2} \quad (17)$$

The densification strain of porous material under quasi-static compression deformation is:

$$\chi_Q = 1 - \phi^i \quad (18)$$

Therefore, the densification strain capacity of the material can be expressed as, Figure 3 shows the mechanical characteristics of porous materials:

$$W = \delta_\phi \chi_Q + 2\rho i^{1/2} \quad (19)$$

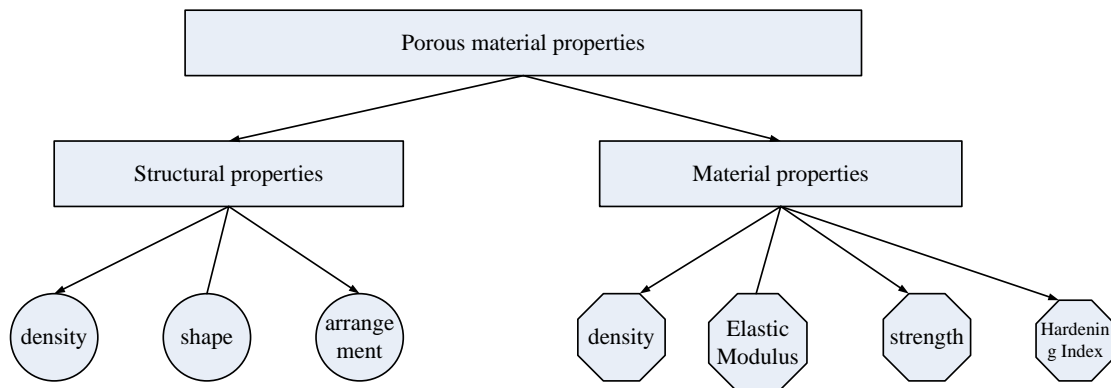


Figure 3. Mechanical characteristics of porous materials

2.3. Micro-nano Photonics

Nanomaterials refer to the morphological structure of matter with a size in the range of 1-100 nm. It is a mesoscopic material between atoms, molecules and macroscopic objects. The comprehensive cross-discipline formed by the combination of nanomaterials-based materials science and other disciplines such as physics, chemistry, biology, etc. has become the forefront of scientific research today, and the resulting nanotechnology and nanoapplication technology have also been obtained rapid development. The novelty of nanomaterials gave birth to micro-nano photonics, which mainly studies the behavior of light at the nanometer scale, focusing on the infrared, visible and ultraviolet bands [19]. Because the size of nanomaterials is equivalent to the wavelength of light, light and sub-wavelength scale substances will produce many new properties, mainly related to the fields of optics, nonlinear optics, and nanomanufacturing [20].

3. Micro-Nano Photonics Building Insulation Material Experiment Based on Porous Material-Based Metal Dielectric Film

3.1. Basic Wall Structure

Due to the large latitude and obvious climate difference between North and South China, the

wall structure in different regions is very different. The wall structure in higher latitudes is mainly made of aerated concrete, and the wall structure in middle and low latitudes is mainly made of reinforced concrete; Common materials in hot summer and cold winter areas include shale hollow brick, aerated concrete, etc [21]. There is a big difference in the wall structure, and there are also differences in the heat transfer performance. The heat transfer performance is mainly manifested in the thermal conductivity [22]. Table 2 shows the advantages and disadvantages of the three types of wall insulation methods:

Table 2. Advantages and disadvantages of the three types of wall insulation

Type	Advantage	Shortcoming
Insulation	Simple operation and low price	Poor water resistance
Sandwich insulation	Less disturbed by the environment	Difficult to install
External insulation	Wide range of adaptation	Affected by the environment

According to the advantages and disadvantages of Table 2, it can be seen that the external thermal insulation is easy to operate, has strong thermal insulation performance, and does not affect the indoor area of the building. It can be promoted in hot summer and cold winter areas; although the external thermal insulation has strong adaptability, the moisture resistance is not bad, However, it is easily affected by the external environment, and the construction is more difficult; sandwich insulation is less disturbed by the external environment, but it is prone to thermal bridges and air convection inside [23].

3.2. Dielectric Film Test Results

It is found through experiments that the relative error of the real part of the dielectric constant does not exceed 3%, and the error of the loss tangent is between 0.05. This data actually demonstrates the feasibility of the coplanar waveguide resonance method in the structure.

Table 3. Dielectric film test results

Resonance frequency f(GHz)	1.329	2.53	3.92
Reference value of real part of dielectric constant (nm)	2.1	2.1	2.1
Tangent loss reference value (nm)	0.0008	0.0008	0.0008
Test value of real part of dielectric constant (nm)	2.41	2.05	2.19
Tangent loss test value (nm)	0.019	0.0047	0.0058
Error (nm)	0.018	0.0049	0.0082

According to the data in Table 3, the relative error of the real part of the dielectric constant of the dielectric film material is very small, almost negligible, and the tangent loss error of the dielectric film is within 0.04 nanometers. According to the test data, the parameters of dielectric film are basically consistent at the resonant frequency point, which shows that the measurement method is effective [24]. Figure 4 is a schematic diagram of the technical route:

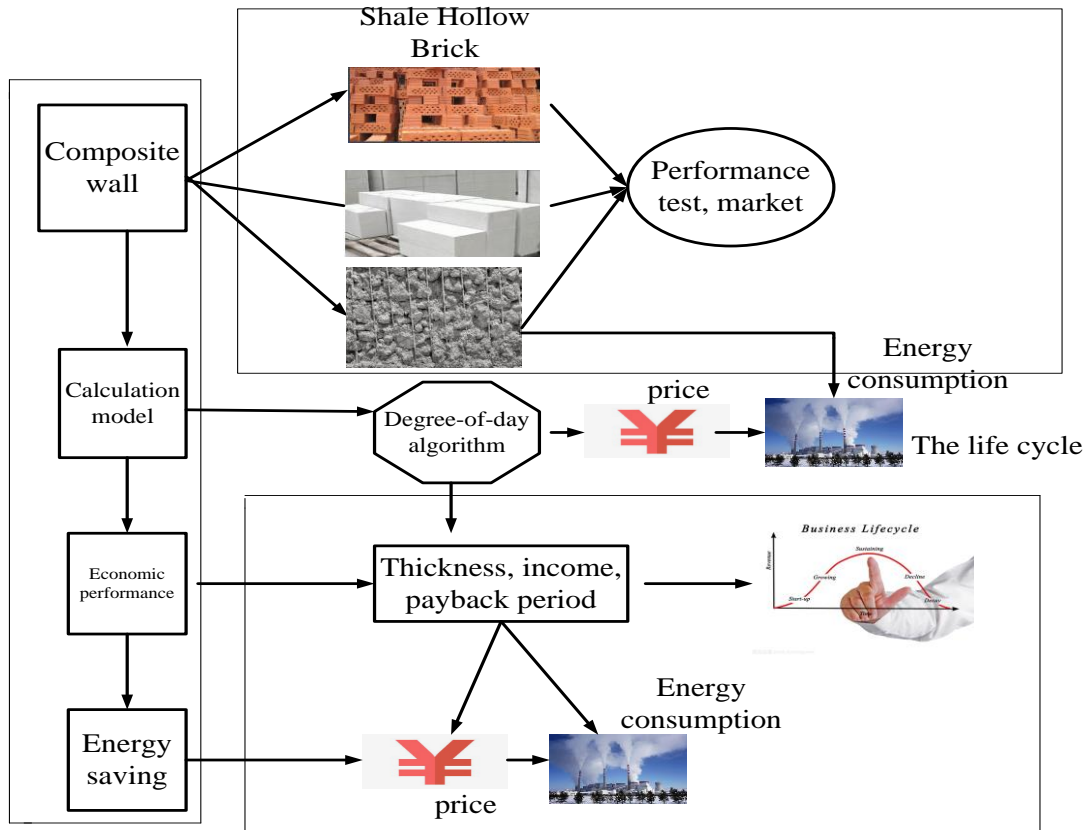


Figure 4. Schematic diagram of technical route

3.3. Test Specimens of Porous Materials

In order to explore the compressive and flexural properties of porous materials, a number of specimens were prepared for the quasi-static compression test and the Tong Taiya collapse test of porous materials. The specific specifications are as follows:

Table 4. Specimen size

Serial number	Ideal size (nm)	Actual size (nm)		
		Long	Width	High
1	0.6*0.6*0.7	60.21	60.32	81.31
2	0.6*0.6*0.7	60.5	60.65	81.43
3	0.6*0.6*0.7	60.3	60.49	80.96
4	0.6*0.6*0.7	60.37	60.71	81.35

According to the data in Table 4, although there is a certain gap between the length and width of the test piece between the actual length and the ideal length, the gap is small from the data size range and is within a reasonable error range. This shows that the difference caused to the material in the processing process is small. However, by comparing the height data of the test piece, it is found that the difference between the actual measured length and the ideal length is about 10%. The main reason for this is that the specimen has a glue step during the processing, and each layer of colloid has a certain thickness, and the overall difference is relatively large [25].

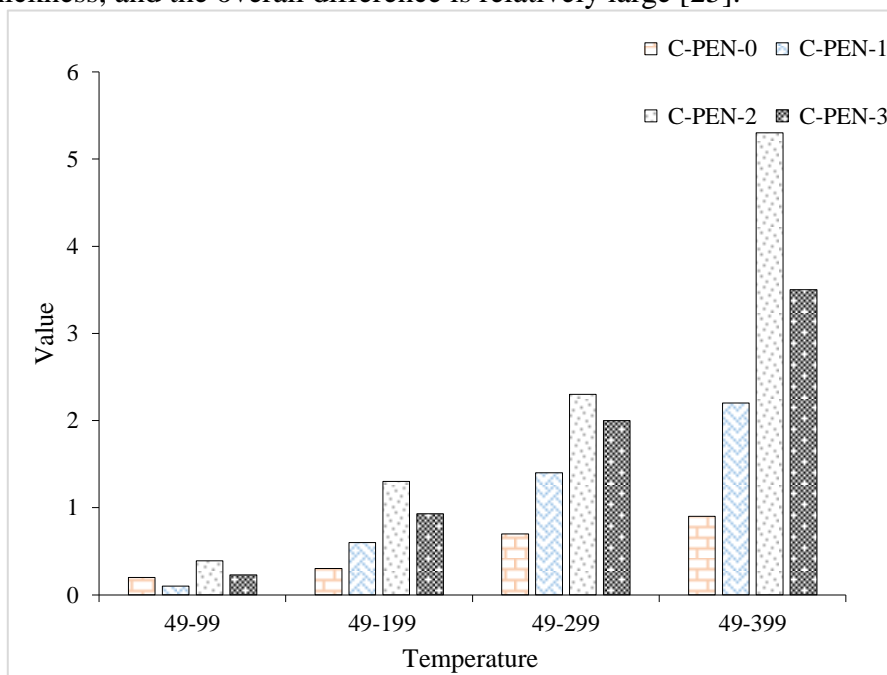


Figure 5. The relationship between dielectric constant and temperature

According to Figure 5, in different temperature ranges, the dielectric constants and temperature numbers of different contents of C-PEN show the same changing trend. Among the four numbers, no matter which temperature range is C- The values of PEN-2 are the largest, which shows that C-PEN-2 is relatively poor in stability. When the temperature is within 299, all c-pen are very stable. From the overall numerical point of view, the stability of c-pen-0 and c-pen-1 is good.

4. Micro-Nano Photonics Building Insulation Materials Based on Porous Material-Based Metal Dielectric Films

4.1. Porous Materials and Temperature Analysis

In this article, glass is used as the main raw material and hollow microspheres are used to prepare porous materials. In order to test the characteristics of porous materials under different temperature conditions, and to further study the influence of different moisture content on the thermal conductivity and the corrosion resistance of the samples, we have The materials were tested.

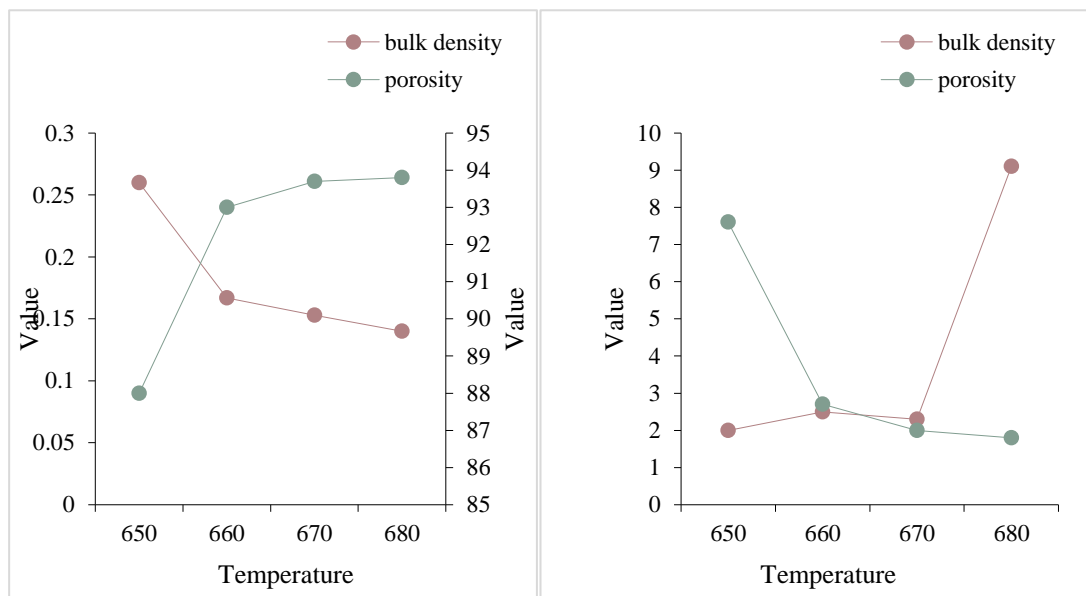


Figure 6. The relationship between porous materials and temperature

According to the data in Figure 6, when the temperature is 650-660, the bulk density of the porous material decreases from 0.26 to 0.17. As the temperature continues to rise, the bulk density of the porous material reaches 0.15 at its lowest, and its porosity is close to 94% at its highest. . Use According to the experimental results, we can think that when the temperature continues to increase, the bulk density of the porous material will continue to decrease. When the temperature is 650-670, the water absorption rate of the porous material does not change significantly. As it rises, the water absorption rate increases rapidly, reaching 9% at the highest point. According to the pressure data, we can see that when the temperature continues to rise, the pressure continues to decrease. When the temperature is in the range of 650-660, the pressure drops rapidly, from 7.6 to 2.7. This trend is the same as the change trend of the bulk density of porous materials [26- 27].

4.2. Relationship between Thermal Conductivity and Bulk Density

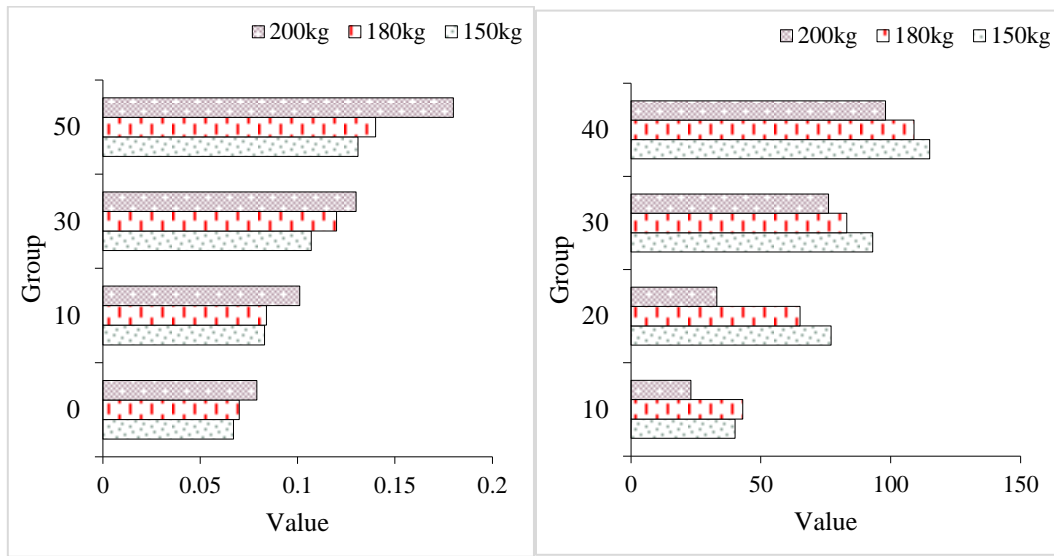


Figure 7. The relationship between sample thermal conductivity and relative saturation

According to the data in Figure 7, when the saturated water absorption rate is the same, the bulk density increases, then the thermal conductivity value of the sample will change accordingly. When the water content is higher, the sample with a large bulk density is higher than the sample with a small bulk density. The growth rate of the thermal conductivity of the sample will be similar to the change of the bulk density. When the saturation is 40%, the growth rate of the bulk density of 150 kg/m³, 180 kg/m³, and 250 kg/m³ is 120%, respectively 123% and 124% [28].

4.3. Insulation System

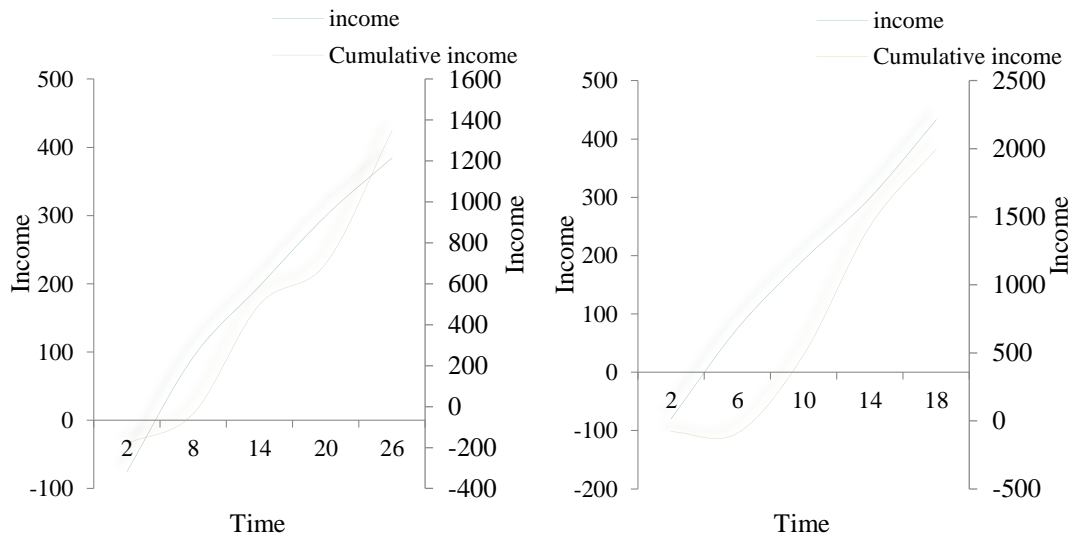


Figure 8. Revenue chart of external temperature system

According to Figure 8, it can be seen from the cumulative income graph (left) that the rock slab began to show positive income in the 10th year after it was put into use, and thereafter, the income showed an upward trend until it reached the life cycle. Because anti-corrosion coatings need to be applied every ten years, the profit chart fluctuates slightly in the tenth, 20th, and 30th years. It can be seen from the figure on the right that the static investment payback period of the polyurethane rigid foam external insulation system (without considering the value of capital) is between 6-7 years, that is, the cost can be recovered in the seventh year, and then until the service life is reached. The time period is in the profitable stage (excluding regular inspection fees and maintenance fees). However, the price is relatively high, and the owners may have some scruples at the initial investment, which may be the biggest obstacle that cannot be widely used at the moment. Promoted by a series of good mechanisms such as improved technology and national policy support in the future, the prospects will continue to improve [29].

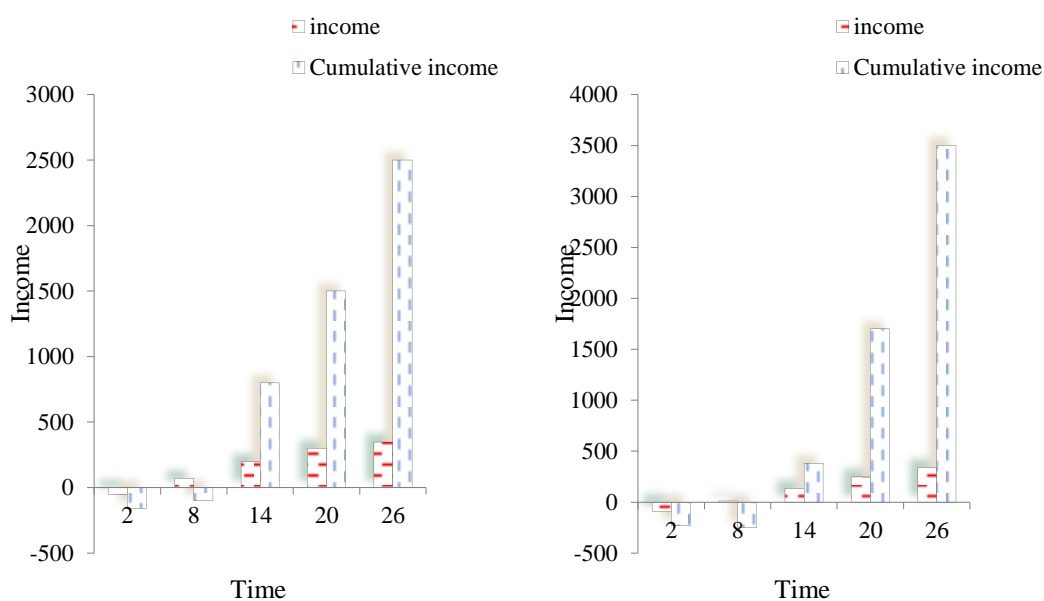


Figure 9. Revenue chart of external temperature system

According to Figure 9, the maintenance cost of the expanded perlite (left) insulation board is relatively low, and the response is not obvious on the profit map. The static investment payback period of expanded perlite external insulation is between 8-9 years, that is, the investment will be recovered in 8-9 years. After that, it will be in a profitable period (excluding regular inspection and maintenance costs). Expanded perlite is a traditional thermal insulation material with a wide range of raw materials, easy to obtain, and low cost, but the thermal insulation effect is general and needs to be improved. Subsequent research mainly focuses on reducing water absorption and reducing thermal conductivity. The static investment payback period of foamed concrete (right) external thermal insulation is between 9-10 years, that is, the investment will be recovered in 9-10 years, and it will be in a profitable period (excluding regular inspection and maintenance costs) [30].

5. Conclusion

As the process of urbanization continues to accelerate, urban architecture is also developing rapidly. Due to the limitation of the material itself, it has brought varying degrees of damage to the

environment and resources. In addition, in recent years, there have been frequent accidents of insulation materials as building materials, and the development of new building materials has become a top priority. This article aims to study the application of micro-nano photonics based on porous material-based metal dielectric membranes in the field of building insulation materials. It is proposed to use glass powder as the main raw material to prepare porous materials using demonstrative technology and spray drying technology. The combination of porous materials and dielectric membrane technology is a new choice of building thermal insulation materials. In this paper, the following tasks are mainly completed: (1) the successful use of waste glass powder has successfully prepared porous materials with small pores, uniform size distribution, high compressive strength, and low thermal conductivity, which has promoted the development of building insulation materials. (2) The porous material is briefly analyzed, and the porous material model is simplified, and the dynamic peak stress of each unit is calculated. (3) Insulation materials have the largest energy consumption in the operational phase of the entire life cycle, followed by energy consumption in the production phase, and the smallest in the transportation and disposal phases. Of course, this paper still has many shortcomings in the experiment, which needs to be improved in the next stage: (1) the porous materials with small pores, uniform size distribution, high compressive strength and low thermal conductivity were successfully prepared by using waste glass powder, which promoted the development of building thermal insulation materials. (2) The basic current situation of building materials is to visit experts in the industry, which is affected by the number and quality of personnel, and the results obtained are not completely universal. (3) The material properties should be further optimized and the thermal conductivity should be reduced. The research on the influence of the thermal conductivity of porous materials is not detailed, and further details are needed.

Funding

This article is not supported by any foundation.

Data Availability

Data sharing is not applicable to this article as no new data were created or analysed in this study.

Conflict of Interest

The author states that this article has no conflict of interest.

References

- [1] Vanson J M , Coudert F X , Klotz M , et al. Kinetic Accessibility of Porous Material Adsorption Sites Studied through the Lattice Boltzmann Method. *Langmuir the Acs Journal of Surfaces & Colloids*, 2018, 33(6):1405-1411. <https://doi.org/10.1021/acs.langmuir.6b04472>
- [2] F Ebrahimi, Jafari A , Barati M R . Vibration analysis of magneto-electro-elastic heterogeneous porous material plates resting on elastic foundations. *Thin-Walled Structures*, 2017, 119(oct.):33-46. <https://doi.org/10.1016/j.tws.2017.04.002>
- [3] Soare, Stefan C . On the overall yielding of an isotropic porous material with a matrix obeying a non-quadratic criterion. *International Journal of Engineering Science*, 2016, 104(JUL.):5-19.

<https://doi.org/10.1016/j.ijengsci.2016.04.005>

- [4] Sadouki M . *Experimental characterization of rigid porous material via the first ultrasonic reflected waves at oblique incidence*. *Applied Acoustics*, 2018, 133(APR.):64-72. <https://doi.org/10.1016/j.apacoust.2017.12.010>
- [5] Hao J H , Chen Q , Kang H . *Porosity distribution optimization of insulation materials by the variational method*. *International Journal of Heat & Mass Transfer*, 2016, 92(JAN.):1-7.
- [6] Osorio J D , Rivera-Alvarez A , Girurugwiro P , et al. *Integration of transparent insulation materials into solar collector devices*. *Solar Energy*, 2017, 147(MAY):8-21. <https://doi.org/10.1016/j.solener.2017.03.011>
- [7] Juan P, Hidalgo, et al. *Experimental Characterisation of the Fire Behaviour of Thermal Insulation Materials for a Performance-Based Design Methodology*. *Fire Technology*, 2016, 53(3):1-32. <https://doi.org/10.1007/s10694-016-0625-z>
- [8] Xu S , Chen L , Gong M , et al. *Characterization and engineering application of a novel ceramic composite insulation material*. *Composites Part B Engineering*, 2017, 111(FEB.):143-147.
- [9] Shin S , Du H , Kim T , et al. *Electron doping and stability enhancement of doped graphene using a transparent polar dielectric film*. *Journal of Materials Science*, 2016, 51(2):748-755. <https://doi.org/10.1007/s10853-015-9397-y>
- [10] Xu W , Ding Y , Yu Y , et al. *Highly foldable PANi@CNTs/PU dielectric composites toward thin-film capacitor application*. *Materials Letters*, 2017, 192(APR.1):25-28. <https://doi.org/10.1016/j.matlet.2017.01.064>
- [11] Chen S , Zhuo B , Guo X . *Large Area One-Step Facile Processing of Microstructured Elastomeric Dielectric Film for High Sensitivity and Durable Sensing over Wide Pressure Range*. *ACS Applied Materials & Interfaces*, 2016, 8(31):20364-20370. <https://doi.org/10.1021/acsami.6b05177>
- [12] Jie, Chen, Hengyu, et al. *Enhancing Performance of Triboelectric Nanogenerator by Filling High Dielectric Nanoparticles into Sponge PDMS Film.* *ACS applied materials & interfaces*, 2016, 8(1):736-44. <https://doi.org/10.1021/acsami.5b09907>
- [13] Yasuda Y , Ueno S , Kadota M , et al. *Applicability of locally reacting boundary conditions to porous material layer backed by rigid wall: Wave-based numerical study in non-diffuse sound field with unevenly distributed sound absorbing surfaces*. *Applied Acoustics*, 2016, 113(dec.):45-57.
- [14] Mo J , Ma W , Zhang W , et al. *Structure and properties of carbon intercalated halloysite and its organosilicone hybrid film with low dielectric constant*. *Materials & Design*, 2017, 128(aug.):56-63. <https://doi.org/10.1016/j.matdes.2017.04.067>
- [15] Tomozeiu N . *Spectroscopic Methods to Investigate Liquid–Porous Material Interactions: An Overview of Optical and Electrical Impedance Techniques*. *Transport in Porous Media*, 2016, 115(3):1-27. <https://doi.org/10.1007/s11242-016-0683-1>
- [16] Song J , Han C , Lai P T . *Comparative Study of Nb2O5, NbLaO, and La2O3 as Gate Dielectric of InGaZnO Thin-Film Transistor*. *IEEE Transactions on Electron Devices*, 2016, 63(5):1-6. <https://doi.org/10.1109/TED.2016.2544439>
- [17] Siddique J , Kara A . *Capillary Rise of Magnetohydrodynamics Liquid into Deformable Porous Material*. *Journal of Applied Fluid Mechanics*, 2016, 9(6):2837-2843. <https://doi.org/10.29252/jafm.09.06.25640>
- [18] S Glodež, S Dervarič, Kramberger J , et al. *Fatigue crack initiation and propagation in lotus-type porous material*. *Frattura E Integrita Strutturale*, 2016, 10(35):152-160.

<https://doi.org/10.3221/IGF-ESIS.35.18>

- [19] Boittin G , Vincent P G , Moulinec H , et al. Numerical simulations and modeling of the effective plastic flow surface of a biporous material with pressurized intergranular voids. *Computer Methods in Applied Mechanics & Engineering*, 2017, 323(aug.15):174-201. <https://doi.org/10.1016/j.cma.2017.05.004>
- [20] Lu G , Fall M . Modelling blast wave propagation in a subsurface geotechnical structure made of an evolutive porous material. *Mechanics of materials*, 2017, 108(MAY):21-39.
- [21] Hmar J , Majumder T , Mondal S P . Growth and characteristics of PbS/polyvinyl alcohol nanocomposites for flexible high dielectric thin film applications. *Thin Solid Films*, 2016, 598(JAN.1):243-251. <https://doi.org/10.1016/j.tsf.2015.12.032>
- [22] Wang X , Tseng L T , Kazazis D , et al. Studying resist performance for contact holes printing using EUV interference lithography. *Journal of Micro/Nanolithography, MEMS, and MOEMS*, 2019, 18(1):013501.1-013501.11.
- [23] Sumislawska M , Gyftakis K N , Kavanagh D F , et al. The Impact of Thermal Degradation on Properties of Electrical Machine Winding Insulation Material. *IEEE Transactions on Industry Applications*, 2016, 52(4):2951-2960.
- [24] Tiso M , Just A . Design criteria for insulation materials applied in timber frame assemblies. *Journal of Structural Fire Engineering*, 2017, 9(3):252-263.
- [25] Hoseini A , Malekian A , Bahrami M . Deformation and thermal resistance study of aerogel blanket insulation material under uniaxial compression. *Energy & Buildings*, 2016, 130(oct.):228-237.
- [26] Rehman H U . Experimental performance evaluation of solid concrete and dry insulation materials for passive buildings in hot and humid climatic conditions. *Applied Energy*, 2017, 185(pt.2):1585-1594.
- [27] Mahapatra M , Karmakar M , Dutta A , et al. Microstructural analyses of loaded and/or unloaded semisynthetic porous material for understanding of superadsorption and optimization by response surface methodology. *Journal of Environmental Chemical Engineering*, 2018, 6(1):289-310. <https://doi.org/10.1016/j.jece.2017.11.078>
- [28] Kram Be Rger J , Sraml M , Glo De Z S . Computational study of low-cycle fatigue behaviour of lotus-type porous material. *International Journal of Fatigue*, 2016, 92(pt.2):623-632. <https://doi.org/10.1016/j.ijfatigue.2016.02.037>
- [29] Tao E , Ying L , Yang S , et al. Nano-montmorillonite-based porous material prepared by gel casting: structure and adsorption properties. *Micro & Nano Letters*, 2017, 13(3):332-334. <https://doi.org/10.1049/mnl.2017.0531>
- [30] Ghose S , Babu S , Van Arkel R J , et al. The influence of laser parameters and scanning strategies on the mechanical properties of a stochastic porous material. *Materials & Design*, 2017, 131(oct.):498-508. <https://doi.org/10.1016/j.matdes.2017.06.041>